Fingerprinting Petroporphyrin Structures with Vibrational Spectroscopy. 4. Resonance Raman Spectra of Nickel(II) Cycloalkanoporphyrins: Structural Effects Due To Exocyclic Ring Size

Roman S. Czernuszewicz,[†,*] J. Graham Rankin,[‡] and Timothy D. Lash[§]

Departments of Chemistry, University of Houston, Houston, Texas 77204, Marshall University, Huntington, West Virginia 25701, and Illinois State University, Normal, Illinois 61790

Received June 15, 1995[⊗]

Nickel(II) complexes of cycloalkanoporphyrins (CAPs) bearing a saturated carbon ring of varying size between pyrrole C_β and methine bridge carbon atoms are widespread in crude oil and related organic rich sediments. We have synthesized a series of NiCAPs containing *meso*,*β*-ethano (NiCAP5), *meso*,*β*-propano (NiCAP6), and *meso*,*β*-butano (NiCAP7) groups and applied UV−visible absorption and resonance Raman (RR) spectroscopies to investigate the effects of the exocyclic ring size on the porphyrin structure and to establish vibrational CAP marker frequencies for petroporphyrins in fossil fuels. The RR spectra of NiCAPs, excited at or near porphyrin Soret (∼400 nm) and Q (510−580 nm) bands are informative and display a rich array of skeletal and alkyl substituent modes. High-frequency (1300−1700 cm^{-1}) structure-sensitive RR bands shift down considerably (up to 24 cm^{-1}) with increasing size of the exocyclic ring, implicating increased nonplanar distortions of the tetrapyrrole macrocycle. Unlike in other petroporphyrins studied thus far, etio- and tetrahydrobenzoporphyrins, out-of-plane distortions of the porphyrin imposed by the *meso*,*β*-cycloalkano ring are also sufficient to destroy the center of symmetry of the porphyrin π-system and produce significant enhancement of the IR-active E_u skeletal modes in the Q-band-excited RR spectra. The UV−visible absorption spectra also vary with the size of the exocyclic ring; both the Soret and Q bands progressively red shift as the cycloalkano chain becomes longer, implying a destabilization of the two highest occupied π orbitals in NiCAP6 and NiCAP7. In addition, the size of the exocyclic ring in NiCAPs can be readily determined from the frequency of the ∼900 cm^{-1} marker band and the characteristic patterns of skeletal and substituent bands in the 700−1200 and ν_4 (∼1380 cm^{-1}) regions.

Introduction

The discovery of metalloporphyrins in crude oil by Alfred Treibs in the mid-1930s[1] provided the first conclusive evidence for the biological origin of petroleum.[2] He tentatively identified two major metalloporphyrins, the oxovanadium(IV) (vanadyl) chelates of etioporphyrin-III (Etio-III) and deoxophylloerythroetioporphyrin (DPEP), and proposed[1b] that these compounds were derived from heme and chlorophyll *a*, respectively. Some 30 years later, mass spectrometric studies[3] revealed that complex mixtures of metalloporphyrins related mainly to Etio-III and DPEP were in fact present in a variety of organic-rich sedimentary materials. Both DPEP[4] and Etio-III[5] have now been isolated from oil shales and unambiguously characterized by nOe difference proton NMR spectroscopy, and the structure of (VO)DPEP has been confirmed by X-ray crystallography.[6] However, many additional porphyrins with diverse carbon skeletons have also been identified,[7−11] and these geological

* To whom correspondence should be addressed.
† University of Houston.
‡ Marshall University.
§ Illinois State University.
⊗ Abstract published in *Advance ACS Abstracts,* November 15, 1995.

(1) Treibs, A. *Justus Liebigs Ann. Chem.* **1934**, *510*, 42−62. (b) Treibs, A. *Angew. Chem.* **1936**, *49*, 682−686.
(2) (a) Baker, E. W.; Palmer, S. E. In *The Porphyrins*; Dolphin, D., Ed.; Academic Press: New York, 1978; Vol. 1, pp 486−552. (b) Baker, E. W.; Louda J. W. In *Biological Markers in the Sedimentary Record*; John, R., Ed.; Elsevier: Amsterdam, 1986; pp 125−225. (c) Callot, H. J. In *The Chlorophylls*; Scheer, H., Ed.; CRC Press, Boca Raton, FL, 1991; pp 339−364.
(3) (a) Baker, E. W. *J. Am. Chem. Soc.* **1966**, *88*, 2311. (b) Baker, E. W.; Yen, T. F.; Dickie, J. P.; Rhodes, R. E.; Clark, L. F. *J. Am. Chem. Soc.* **1967**, *89*, 3631.
(4) (a) Quirke, J. M. E.; Maxwell, J. R.; Eglinton, G.; Sanders, J. K. M. *Tetrahedron Lett.* **1980**, *21*, 2987−2990. (b) Fookes, C. J. R. *J. Chem. Soc., Chem. Commun.* **1983**, 1472−1473. (c) Shulga, A. M.; Serebrennikova, O. V.; Mozzhelina, T. K. *Neftekhimiya* **1986**, *26*, 309.
(5) (a) Quirke, J. M. E.; Maxwell, J. R. *Tetrahedron* **1980**, *36*, 3453. (b) Fookes, C. J. R. *J. Chem. Soc., Chem. Commun.* **1985**, 703. (c) Chicarelli, M. I.; Wolff, G. A.; Maxwell, J. R. *J. Chem. Soc., Chem. Commun.* **1985**, 723.
(6) (a) Ekstrom, A.; Fookes, C. J. R.; Hambley, T.; Loeh, H. J.; Miller, S. A.; Taylor, J. C. *Nature* **1983**, *306*, 173−174. (b) Pettersen, R. C. *Acta Crystallogr., Sect. B* **1969**, *25*, 2527−2539.
(7) (a) Filby, R. H.; Van Berkel, G. J. In *Metal Complexes in Fossil Fuels. Geochemistry, Characterization, and Processing;* Filby, R. H., Branthaver, J. F., Eds.; American Chemical Society: Washington DC, 1987; pp 2−39. (b) Chicarelli, M. I.; Kaur, S.; Maxwell, J. R. *Ibid.,* pp 40−67. (c) Ocampo, R.; Callot, H. J.; Albrecht, P. *Ibid.,* pp 68−73.
(8) (a) Callot, H. J.; Ocampo, R.; Albrecht, P. *Energy Fuels* **1990**, *4*, 635−639. (b) Verne-Mismer, J.; Ocampo, R.; Bauder, C.; Callot, H. J.; Albrecht P. *Energy Fuels* **1990**, *4*, 639−643. (c) Keely, B. J.; Prowse, W. G.; Maxwell, J. R. *Energy Fuels* **1990**, *4*, 628−638. (d) Eckardt, C. B.; Keely, B. J.; Waring, J. R.; Chicarelli, M. I.; Maxwell, J. R. *Philos. Trans. R. Soc. London B* **1991**, *333*, 339−348. (e) Ocampo, R.; Bauder, C.; Callot, H. J.; Albrecht, P. *Geochim. Cosmochim. Acta* **1992**, *56*, 745−761.
(9) (a) Wolff, G. A.; Murray, M.; Maxwell, J. R.; Hunter, B. K.; Sanders, J. K. M. *J. Chem. Soc., Chem. Commun.* **1983**, 922−924. (b) Fookes, C. J. R. *J. Chem. Soc., Chem. Commun.* **1983**, 1474−1476. (c) Storm, C. B.; Krane, J.; Skjetne, T.; Telnaes, N.; Branthaver, J. F.; Baker, E. W. *Science* **1984**, *223*, 1075−1076. (d) Chicarelli, M. I.; Maxwell, J. R. *Tetrahedron Lett.* **1984**, *25*, 4701−4704. (e) Chicarelli, M. I.; Wolff, G. A.; Murray, M.; Maxwell, J. R. *Tetrahedron* **1984**, *40*, 4033−4035. (f) Chicarelli, M. I.; Maxwell, J. R. *Tetrahedron Lett.* **1986**, *27*, 4653−4654. (g) Prowse, W. G.; Chicarelli, M. I.; Keely, B. J.; Kaur, S.; Maxwell, J. R. *Geochim. Cosmochim. Acta* **1987**, *51*, 2875−2877. (h) Prowse, W. G.; Maxwell, J. R. *Geochim. Cosmochim. Acta* **1989**, *53*, 3081−3089.
(10) (a) Verne-Mismer, J.; Ocampo, R.; Callot, H. J.; Albrecht P. *J. Chem. Soc., Chem. Commun.* **1987**, 1581−1583. (b) Kaur, S.; Chicarelli, M. I.; Maxwell, J. R. *J. Am. Chem. Soc.* **1986**, *108*, 1347−1348.

0020-1669/96/1335-0199$12.00/0

pigments, generally called geoporphyrins or petroporphyrins, have emerged as unique and sensitive indicators of the paleodepositional environment and diagenetic (time−temperature) history of the sedimentary rocks important to petroleum exploration.[2b,8e,12] For example, comparisons of paleoenvironmental parameters, organic geochemical biomarkers, and petroporphyrin distributions have shown that certain porphyrin distributions can be used to distinguish lacustrine, hypersaline lacustrine, and marine depositional environments.[12c−h]

In oil shales and petroleum, petroporphyrins occur almost exclusively as the nickel(II) and vanadyl complexes, although metal-free porphyrins[8b,13] and traces of iron[14] and copper(II)[8b,15] porphyrins have been detected in immature sediments. The most widespread structural type of petroporphyrins contains a saturated carbon exocycle (five to seven carbons) between a pyrrole β-carbon and the *meso*-carbon of the tetrapyrrole macrocycle (Figure 1). This family of petroporphyrins is collectively known as cycloalkanoporphyrins (CAPs). Among these, the skeletons with five-membered exocyclic rings (a−f) predominate, primarily because the chlorophylls are major biological precursors to fossil porphyrin pigments.[2] The origin of the most common CAP, DPEP (a), is now well established as the degradation product of chlorophyll *a* by a series diagenetic steps often referred to as the "Treibs scheme" after Alfred Treibs who first proposed them 60 years ago.[1b] Several modifications to the original proposal have been made based on more recent studies of petroporphyrins in sediments of very low maturity giving rise to a modified Treibs scheme.[2b] The origin of other less abundant CAPs including *meso*,β-propanoporphyrins (CAP6s) (g) and *meso*,β-butanoporphyrins (CAP7s) (h) are still a subject of debate. Cyclization of the propionic acid side chain at position C-17 in chlorophylls has been proposed as the source of CAP7s.[9b] The formation of 15^1-methyl CAP6s is more enigmatic. The only known biological tetrapyrrolic pigment containing a six-membered exocyclic ring is the nickel archaebacterial pigment Factor F_{430}.[16] However, if this compound were the source of CAP6 petroporphyrins, then extensive and regioselective loss of multiple functional groups and alkyl substituents would be required. In addition, the selective introduction of a methyl substituent on the six-membered exocyclic ring would be needed. A more likely possibility is that a common intermediate leading to the CAP7s undergoes a carbocation rearrangement that results in a ring contraction.[17] The ability to determine the structures of the minor porphyrin components will be crucial in identifying the sources and diagenetic pathways leading to the final sedimentary tetrapyrroles.

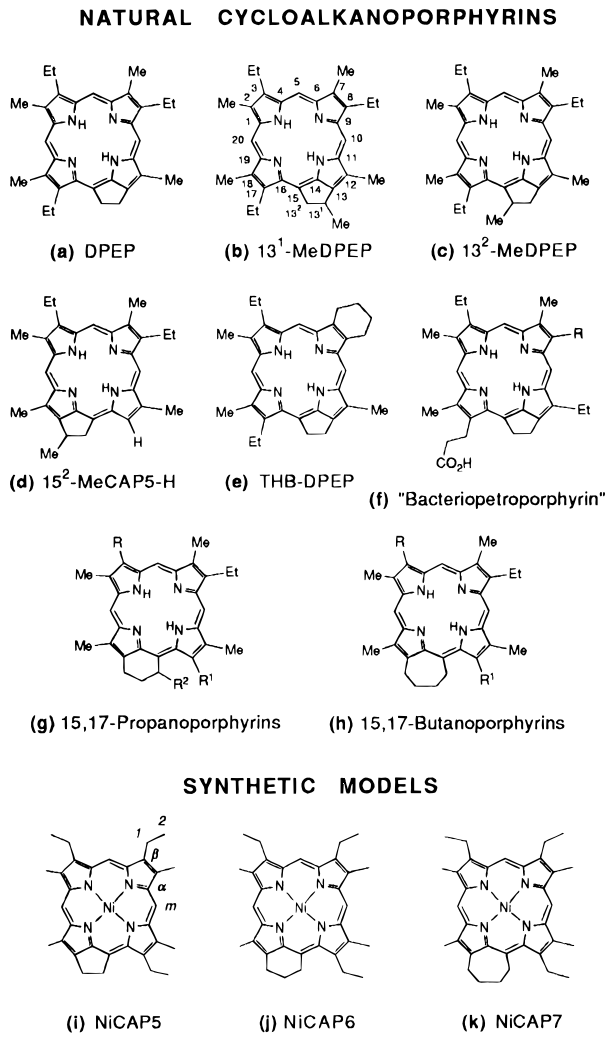

Figure 1. Representative cycloalkanoporphyrins from geological sources (a−h) and their synthetic models studied in this work (i−k). *Natural petroporphyrins* usually occur in the form of the vanadyl (primarily) or nickel(II) chelates: R = H, CH_3, or CH_2CH_3; R_1 = H, CH_3, or CH_2CH_3; R_2 = H or CH_3. DPEP[1] (a) and its 13^1-methyl[7b] (b), 13^2-methyl[7d] (c), and 7,8-butano (tetrahydrobenzo-DPEP[10]) (e) derivatives, like chlorophyll *a*, have the five-membered ring exocyclic between carbons 13 and 15, right side, whereas larger ring sizes are located on the left side between carbons 15 and 17 (g, h). *Synthetic models*, the synthetic NiCAPs used in this work (i−k), are symmetrical on the top half and hence the exocycle can be considered either on the left or right side, and a left convention was chosen throughout this work. These CAPs can also be considered derivatives of Etio-II in that the relative arrangements of methyl and ethyl substituents are the same.

Spectroscopic probes of petroporphyrin structure are needed to aid in determining and differentiating the numerous porphyrins known to exist in petroleum and related deposits. In this regard, resonance Raman (RR) spectroscopy has been particularly successful in elucidating metalloporphyrin structural features and dynamics,[18] including the effects of the porphyrin's central metal and peripheral substituents upon the conformation of the macrocycle. Previously, we showed[19] that the strongest RR band in the Soret-excited spectrum of (VO)Etios arises from the characteristic vanadyl stretch at 991 cm^{-1} and that many

(11) (a) Ocampo, R.; Callot, H. J.; Albrecht, P.; Kintzinger, J. P. *Tetrahedron Lett.* **1984**, *25*, 2589−2592. (b) Ocampo, R.; Callot, H. J.; Albrecht, P. *J. Chem. Soc., Chem. Commun.* **1985**, 200−201.

(12) (a) Baker, E. W.; Louda, J. W.; Orr, J. W. *Org. Geochem.* **1987**, *11*, 303−309. (b) Lipiner, G.; Willner, I.; Aizenshtat, Z. *Org. Geochem.* **1988**, *13*, 747−756. (c) Peng, P.; Eglinton, G.; Fu; J.; Sheng, G. *Energy Fuels* **1992**, *6*, 215−225. (d) Sundararaman, P.; Dahl, J. E. *Org. Geochem.* **1993**, *20*, 333−337. (e) Keely, B. J.; Maxwell, J. R. *Org. Geochem.* **1993**, *20*, 1217−1225. (f) Sundararaman, P.; Boreham, C. J. *Geochim. Cosmochim. Acta* **1993**, *57*, 1367−1377. (g) Sundararaman, P.; Moldowan, J. M. *Geochim. Cosmochim. Acta* **1993**, *57*, 1379−1386. (h) Sundararaman, P. *Geochim. Cosmochim. Acta* **1993**, *57*, 4517−4520. (i) Ocampo, R.; Riva, A.; Trendel, J. M.; Riolo, J.; Callot, H. J.; Albrecht, P. *Energy Fuels* **1993**, *7*, 191−193. (j) Serebrennikova, O. V.; Mozzhelina, T. K. *Org. Geochem.* **1994**, *21*, 891−895.

(13) Palmer, S. E.; Baker, E. W. *Science* **1978**, *201*, 49. (b) Baker, E. W.; Louda, J. W. *Org. Geochem.* **1984**, *6*, 183.

(14) Baker, E. W.; Palmer, S. E.; Huang, W. Y. *Initial Rep. Deep Sea Drill. Proj.* **1978**, *41*, 825−837.

(15) Chicarelli, M. I.; Eckardt, C. B.; Owen, C. R.; Maxwell, J. R.; Eglington, G.; Hutton, R. C.; Eaton, A. N. *Org. Geochem.* **1990**, *15*, 267.

(16) (a) Pfaltz, A.; Jaun, B.; Fassler, A.; Eschenmoser, A.; Jaenchen, R.; Gilles, H. H.; Diekart, G.; Thaurer, R. K. *Helv. Chim. Acta* **1982**, *65*, 828−865. (b) Kaplan, W. A., Suslick, K. S.; Scott, R. A. *J. Am. Chem. Soc.* **1991**, *113*, 9824−9827.

(17) Lash, T. D.; Balasubramaniam, R. P. *Tetrahedron Lett.* **1990**, *31*, 7545−7548.

(18) (a) Spiro, T. G.; Li, X.-Y. In *Biological Applications of Raman Spectroscopy*, Spiro, T. G., Ed.; Wiley: New York, 1988; Vol. 3, pp 1−38. (b) Spiro, T. G.; Czernuszewicz, R. S.; Li, X.-Y. *Coord. Chem. Rev.* **1990**, *100*, 541−571.

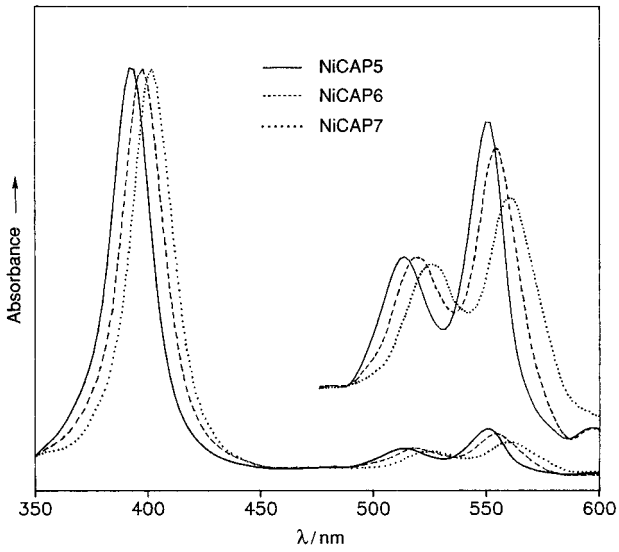

Figure 2. UV−visible spectra of nickel(II) complexes of CAP5, CAP6, and CAP7 in CH_2Cl_2 solution (normalized to Soret band). Conditions: average of three scans each; resolution, 2 nm.

(VO)Etio high-frequency vibrations associated mainly with pyrrole $C_\beta C_\beta$ and methine bridge $C_\alpha C_m$ stretching modes have significantly lower (14−28 cm^{-1}) frequencies than their corresponding modes in NiEtios, enabling the two petroporphyrin families to be readily distinguished. We have also demonstrated the potential of RR spectroscopy, especially with the porphyrin Q-band absorption excitation, to differentiate petroporphyrin positional isomers via significant differences in the 750−1050 cm^{-1} alkyl substituent vibrations of NiEtio isomers I−IV.[19,20] In another recent study, we established structure marker bands unique to tetrahydrobenzoetioporphyrins, assigned vibrational modes related to the tetrahydrobenzo exocyclic ring, and showed that RR spectroscopy can distinguish petroporphyrin positional isomers possessing the same overall symmetry.[21]

In this paper, the question of *meso*,*β*-alkano exocyclic ring involvement in the NiCAP vibrational spectra is examined for the first time using resonance Raman spectroscopy. Both the Soret- and Q-band excitation were used to obtain high-quality RR spectra of the nickel(II) complexes of *meso*,*β*-ethano- (NiCAP5), *meso*,*β*-propano- (NiCAP6), and *meso*,*β*-butano-porphyrins (NiCAP7). UV−visible absorption spectra of the three metalloporphyrins were also obtained, which reveal a systematic bathochromic shift of the Soret and Q bands with increasing size of the *meso*,*β*-alkano exocycle. Specific Raman modes that are perturbed by this type of petroporphyrin structural motif and that distinguish each of the NiCAPs are identified. In particular, the increase in size of the cycloalkano exocyclic ring leads to a decrease in the porphyrin π-conjugation which in turn causes a decrease in the frequency of the porphyrin structure-sensitive vibrational modes. The RR spectra also can be used to identify the NiCAPs and to elucidate the conformational differences between them.

Experimental Section

Materials and Methods. The syntheses of the free-base cycloalkanoporphyrins used in this work, H_2CAP5 = 15,17-ethano-3,7,13-triethyl-2,8,12,18-tetramethylporphyrin, H_2CAP6 = 15,17-propano-3,7,13-triethyl-2,8,12,18-tetramethylporphyrin, H_2CAP7 = 15,17-butano-3,7,13-triethyl-2,8,12,18-tetramethylporphyrin, have been previously reported.[22−24] The nickel complexes were obtained by refluxing the corresponding free-base porphyrin with nickel acetate in dimethylformamide[25] followed by thin layer chromatography (Absorbosil from Alltech, 250 μm, developed with carbon disulfide). The RR spectra were obtained with a Coherent K-2 Kr^+ ion laser excited at or near the absorption maxima of the porphyrin Soret and Q bands with 406.7 (violet), 530.9 (green), and 568.2 nm (yellow) lines. Essentially all of the Raman-active fundamental modes can be identified in the spectra by using these three excitation wavelengths, as previously demonstrated by studies of Ni complexes of octaethylporphyrin (OEP),[26] *meso*-tetraphenylporphyrin (TPP),[27] etioporphyrins I−IV,[19,20] and four isomeric tetrahydrobenzoporphyrins (THBP).[21] The scattered photons were collected via backscattering geometry from spinning NMR tubes[28] in solution (∼1 mM in carbon disulfide). Conventional scanning Raman instrumentation equipped with a Spex 1403 double monochromator and a Hamamatsu 928 photomultiplier detection system was used to record the spectra under the control of a Spex DM3000 microcomputer system.[29] Raman data were obtained at 0.5-cm^{-1} increments with integration times of 1 s per point for all spectra. Three scans were averaged to improve signal to noise ratios. Raman data manipulation was performed using LabCalc software (version A2.23; Galactic Industries, Inc.) on a 486-DX 33 MHz PC microcomputer. Solvent bands were routinely subtracted using reference spectra collected under identical conditions of scan rate and slit width utilizing the LabCalc subroutines. The quality of the observed Raman signal in most scans was sufficiently high that baseline correction or smoothing were required only for Q-band low frequency region and all the plots shown in this work are on the uncorrected data. A Hewlett-Packard 8-pen ColorPro graphics plotter was used for hard copy output of spectra.

Optical absorption spectra were obtained in methylene chloride with 1-mm quartz cell using an HP-8542 diode array spectrophotometer. The concentration of each metalloporphyrin was adjusted such that the maximum absorbance (Soret) was about 1 absorbance unit. Resolution of the diode array was 2 nm; however, reproducibility of the absorption maxima wavelengths, both Soret and Q bands, were found to be better than 0.2 nm. Three spectra at 1 s integration time each were averaged.

Table 1. UV−Visible Absorption Maxima (nm) and Relative Absorbances for Nickel Complexes of Cycloalkanoporphyrins[a]

	λ_{max}			absorbance ratio		
porphyrin	Soret	Q_1	Q_0	Soret/Q_1	Soret/Q_0	Q_0/Q_1
NiCAP5[b]	392.9	513.7	550.5	18.88	9.74	1.94
NiCAP6	397.7	520.0	554.8	19.23	10.79	1.78
NiCAP7	402.8	526.5	561.0	20.13	13.73	1.47

[a] Spectra in methylene chloride solution. [b] Numbers indicate the size of the *meso*,*β*-alkano ring.

(19) Rankin, J. G.; Czernuszewicz, R. S. *Org. Geochem.* **1993**, *20*, 521−538.
(20) Rankin, J. G.; Czernuszewicz, R. S.; Lash, T. D. *Org. Geochem.* **1995**, *23*, 419−427.
(21) Rankin, J. G.; Czernuszewicz, R. S.; Lash, T. D. *Inorg. Chem.* **1995**, *34*, 3025−3037.
(22) (a) Lash, T. D. In *Advances in Nitrogen Heterocycles*; Moody, C. J., Ed.; JAI Press Inc.: New York, 1995; Vol. 1, pp 19−69. (b) Lash, T. D.; Balasubramaniam, R. P.; Catarello, J. J.; Johnson, M. C.; May, D. A., Jr.; Bladel, K. A.; Feeley, J. M.; Hoehner, M. C.; Marron, T. G.; Nguyen, T. H.; Perun, T. J., Jr.; Quizon, D. M.; Shiner, C. M.; Watson, A. *Energy Fuels* **1990**, *4*, 668−674. (c) Lash, T. D. *Org. Geochem.* **1989**, *14*, 213−225.
(23) (a) Lash, T. D.; Quizon-Colquitt, D. M.; Shiner, C. M.; Nguyen, T. H.; Hu, Z. *Energy Fuels* **1993**, *7*, 172−178. (b) Lash, T. D.; Catarello, J. J. *Tetrahedron* **1993**, *49*, 4159−4172. (c) Quizon-Colquitt, D. M.; Lash, T. D. *J. Heterocycl. Chem.* **1993**, *30*, 477−482.
(24) (a) Lash, T. D. *Tetrahedron Lett.* **1988**, *29*, 6877−6880. (b) Lash, T. D.; Johnson, M. C. *Tetrahedron Lett.* **1989**, *30*, 5697−5698. (c) Lash, T. D.; Bladel, K. A.; Shiner, C. M.; Zajeski, D. L.; Balasubramaniam, R. P. *J. Org. Chem.* **1992**, *57*, 4809−4820. (d) Bastian, J. A.; Lash, T. D. Manuscript in preparation.
(25) Adler, A. D.; Longo, F. R.; Kampas, F.; Kim, J. *J. Inorg. Nucl. Chem.* **1970**, *32*, 2443−2445.
(26) Li, X.-Y.; Czernuszewicz, R. S.; Kincaid, J. R.; Stein, P.; Spiro, T. G. *J. Phys. Chem.* **1990**, *94*, 47−61.
(27) Li, X. -Y.; Czernuszewicz, R. S.; Kincaid, J. R.; Su, Y. O.; Spiro, T. G. *J. Phys. Chem.* **1990**, *94*, 31−47.
(28) (a) Walters, M. A. *Appl. Spectrosc.* **1983**, *37*, 299−300. (b) Eng, J. F.; Czernuszewicz, R. S.; Spiro, T. G. *J. Raman Spectrosc.* **1985**, *16*, 432−437.
(29) Czernuszewicz, R. S. In *Methods in Molecular Biology*; Jones, C., Mulloy, B., Thomas, A. H., Eds.; Humana Press: Totowa, NJ, 1993; Vol. 17, Chapter 15, pp 345−374.

Table 2. Observed RR Frequencies (cm^{-1}) and Assignments for Ni(II) Complexes of Etio-II and Cycloalkanoporphyrins: CAP5, CAP6, and CAP7[a]

	RR frequencies				
ρ	Etio-II	CAP5	CAP6	CAP7	assignment
dp[b]	1655	1651	1645	1640	ν_{10} (B_{1g})
p	1607	1607	1603	1596	ν_2 (A_{1g})
ap			1603	1601	ν_{37} (E_u) [c]
ap	1603	1595	1583	1578	ν_{19} (A_{2g})
dp	1579	1576	1574	1570	ν_{11} (B_{1g})
ap		1554	1535	1528	ν_{38} (E_u)
p	1522	1535	1515	1511	ν_3 (A_{1g})
p		1484/1499/1520	1482/1492	1475/1490	CH_2 scis-R; CH_3 def-Et,Me[d]
ap		1486[e]	1486		CH_2 scis-R; CH_3 def-Et,Me
ap		1486[e]	1489	1482	ν_{39} (E_u)
dp	1483	1482	1480	1474	ν_{28} (B_{2g})
ap	1463	1465			CH_2 scis-Et
p		1443/1434/1420	1437/1426	1439/1423	CH_2 scis-Et
dp	1409	1403	1410	1408	ν_{29} (B_{2g})
ap	1398	1398	1398	1397	ν_{20} (A_{2g})
dp			1383sh	1384	ν_{12} (B_{1g})
p	1381	1379	1381	1376	ν_4 (A_{1g})
dp		1370	1370	1370	CH_3 umb-Me
p	1368	1367		1371	CH_3 umb-Me
ap	1361	1361[e]			CH_3 umb-Me
ap		1361[e]	1362	1363	ν_{41} (E_u)
p		1347/1359	1348	1340/1323	CH_2 wag-R
ap		1347	1348	1343	CH_2 wag-R
ap			1327/1318	--	CH_2 wag-R
p	1310	1310	1310	1312	CH_2 wag-Et
ap		1310	1310	--	CH_2 wag-Et
ap	1305	1284	1284	1284	ν_{21} (A_{2g})
ap	1268	1267	1267	1266	CH_2 twist-Et
p	1258	1257/1267/1278	1255/1248	1264/1255	CH_2 twist-Et
p		1240	1241	1243	CH_2 twist-R
dp	1226	1227	1226	1225	ν_{13} (B_{1g})
p		1178	1194	1178	ν_5 (A_{1g})-R
dp		1178	1186	1174	ν_{14} (B_{1g})-R
dp	1160	1155	1162	1157	ν_{30} (B_{2g})
dp		1143	1146	1146	ν_{14} (B_{1g})-Et,Me
p	1136	1129/1138	1135/1146	1137/1133	ν_5 (A_{1g})-Et,Me
ap	1120	1121	1117	1118	ν_{22} (A_{2g})
ap			1126	1128	ν_{44} (E_u)
p	1098	1107	1113	1098	CH_3 rock-Et,Me
ap	1099	1089		1098	CH_3 rock-Et,Me
ap	1059	1059	1058	1060	ν_{23} (A_{2g})
p	1059	1054	1054	1054	CH_3 rock
dp			1044/1029	1026	ν(CC)-R
dp	1010	1001[e]	1001[e]	1001	ν_{31} (B_{1g})
dp	999	1001[e]	1001[e]	998	ν(CC)-Et
p	989	995/989	998/989	998/985	ν(CC)-Et
p		973	976	952	CH_3 rock-Et,Me
dp	948	942	931	927	ν_{32} (B_{2g})
ap	918	919	924	920	CH_3 rock-Me
p		904	883	883/888	ν(CC)-R
p	845	829	841/862	840	γ_{10} (B_{1u}), $\gamma(C_mH)$
ap	837		835	837	γ_{19} (E_g), $\gamma(C_mH)$
p	815	818	818	820	ν_6 (A_{1g})
dp		785/799	780	786	CH_2 rock-Et,R
p	782	767/796	769/796/807	769	CH_2 rock-Et,R
dp	751	757	758	756	ν_{15} (B_{1g})
dp	753		753		ν_{16} (B_{1g})
dp	737	733	733	734	γ_5 (A_{1u}), Pyr fold
p	676	705	705	707	ν_7 (A_{1g})
p		716	714	725	CH_2 rock-R
dp		679	680	681	CH_2 rock-R
p		619	615/610/605	595	$\delta(C_\beta C_1 C_2)$-R
p		584/599	593	584	$\delta(C_\beta C_1 C_2)$-R
ap	593	584	593		ν_{24} (A_{2g})
ap	553	555	558	557	ν_{25} (A_{2g})
p	562	555	558/567	552	δ_5 (E_g), $\gamma(C_\beta C_1 C_2)_{asym}$
p	519	512	509/495	512	δ_2 (A_{2u}), $\gamma(C_\beta C_1 C_2)_{sym}$
dp	498/488	498	485	486	ν_{33} (B_{2g})
p		485/443	478/450	486/453	$\delta(C_\beta C_1 C_2)$-R
p	408/382	419/403	415/411	413	δ_4 (B_{2u}), $\gamma(C_\beta C_1 C_2)$-Et
dp			405		$\delta(C_\beta C_1 C_2)$-R
p	363	377	382/369	394	$\delta(C_\beta C_1 C_2)$-Et

Table 2 (Continued)

	RR frequencies				
ρ	Etio-II	CAP5	CAP6	CAP7	assignment
p	353	354	354	361	γ_6 (A_{2u}), Pyr tilt
p	341	342	342/325	344/361/320	ν_8 (A_{1g})
p		315	316	315	ν_{51} (E_g)
p	258	272/265	276/272	280/258	ν_9 (A_{1g})
p	229	229	234	255/230	γ_{24} (A_{2u})
p		198			
dp	198	206	199	201	ν_{34} (B_{1g})
dp	170		168		ν_{18} (B_{1g})

[a] Observed values from CS_2 and CH_2Cl_2 (600−700 cm^{-1}) solution RR spectra at room temperature. Assignments based on normal coordinate analysis for NiOEP[26,38b] and NiEtio-I.[42] [b] Key: p = polarized, dp = depolarized, and ap = anomalously polarized bands. [c] IR active modes, tentative assignment. [d] Key: scis = scissors, umb = umbrella, wag = wagging, twist = twisting, rock = rocking, def = deformation, and ν(CC) stretching modes of the ethyl (Et) and methyl (Me) groups and exocyclic rings (R). [e] Overlapping bands.

Results and Discussion

1. Electronic Spectra and RR Enhancement. The UV−visible spectra of NiCAPs follow that of the classical nickel alkyl porphyrins[30] with a strong Soret band and two Q bands in the deep violet and green-yellow regions, respectively. Figure 2 compares the absorption spectra of NiCAP5, NiCAP6, and NiCAP7 in CH_2Cl_2 solution. The peak maxima (λ_{max}) and relative absorbance ratios are given in Table 1. There is a bathochromic shift of about 5−6 nm for both the Soret and Q_1 bands going from five to six member rings and six to seven. The Q_0 band also shifts to lower energies with increasing ring size but less for 5−6 (∼4 nm) than 6−7 (∼6 nm). A progresive broadening of the Soret (by ∼1 nm) and Q bands (by ∼3 nm) is noted for the series (Figure 2). Also, the intensities of the Q bands decrease relative to the Soret band as the cycloalkano ring becomes larger; the Q_0 band also loses intensity relative to the Q_1 band (Table 1). The bathochromic shift of the absorption spectrum is expected with increasing nonplanarity of the porphyrin macrocycle.[31] A similar shift but smaller is observed between NiCAPs with increasing alkyl chain length at position 13.[32] As there is no change in the number of electrons in the π cloud (i.e. no additional conjugation from, for example, such substituents as the vinyl groups in protoporphyrin IX), the loss of overlap of the π-bonds by the distortion of the macrocycle raising the HOMO, but not the LUMO, could be a possible mechanism for the bathochromic shift.[33]

The pattern of resonance enhancement is similar to those of NiEtios[19,20] and NiTHBPs[21] with polarized (p) bands dominating the 406.7-nm (violet), anomalously polarized (ap) bands the 530.9-nm (green), and depolarized (dp) bands the 568.2-nm (yellow) excitation spectra. Like for NiEtios and NiTHBPs, the 700−1200-cm^{-1} region with yellow excitation is most informative with respect to alkyl modes,[20] their strong enhancement allowing identification of several CAP structure marker bands. These are discussed in detail below. All observed bands for the nickel complexes of CAP5, CAP6, and CAP7 are given in Table 2 along with NiEtio-II as a comparison. A number of new bands not seen in NiEtios and NiTHBPs are located, especially several moderately strong ap bands in the regions around 1120, 1300−1370, and 1500−1600 cm^{-1}. Assignments have been made based on band wavenumber, polarization, enhancement pattern, and relative intensity by comparison to those of NiEtios[19] and NiOEP.[26]

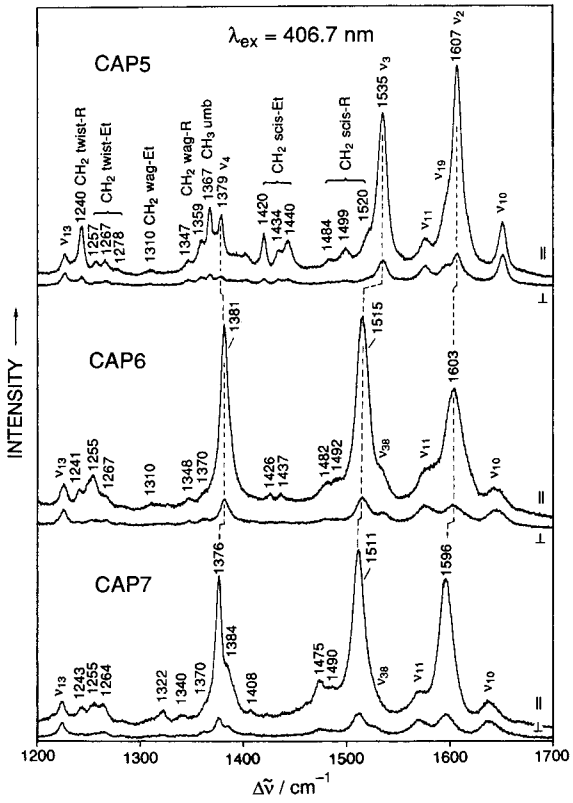

Figure 3. 406.7-nm-excited RR spectra in parallel (∥) and perpendicular (⊥) scattering of Ni(II) complexes of CAP5 (top), CAP6 (middle), and CAP7 (bottom) (∼1 mM) in CS_2 in the 1200−1700-cm^{-1} region, where the most prominent porphyrin structure-sensitive vibrations occur. Conditions: backscattering from spinning NMR tube; 150-mW laser power; 3-cm^{-1} slit widths; average of three scans, each scan with 1-s integration time per data point at 0.5-cm^{-1} increments. Polarized (A_{1g}) bands are correlated.

2. In-Plane Skeletal Modes and Structure in Solution. a. The 1200−1700-cm^{-1} Region. Figures 3−5 compare the RR spectra of nickel complexes of CAP5, CAP6, and CAP7 in the 1200−1700-cm^{-1} region, obtained in CS_2 solution with 406.7-, 530.9-, and 568.2-nm laser lines, respectively, where the many porphyrin structure-sensitive marker bands occur. The observed frequencies for all in-plane porphyrin skeletal modes of the three cycloalkanoporphyrins are tabulated in Table 3. Also given in Table 3, for comparison purposes, are the NiEtio-II in-plane skeletal RR frequencies and the NiEtio-I 1100−1600 cm^{-1} IR frequencies (E_u modes). In general, the porphyrin skeletal modes show some sensitivity to the presence of the exocyclic ring in the three NiCAP structures. A comparison of the NiCAP5 and NiEtio-II vibrational modes reveals that most of

(30) Gouterman, M. In *The Porphyrins*; Dolphin, D., Ed.; Academic Press: New York, 1978; pp 1−165.
(31) (a) Alden, R. G.; Crawford, B. A.; Doolen, R.; Ondrias, M. R.; Shelnutt, J. A. *J. Am. Chem. Soc.* **1989**, *111*, 2070−2072. (b) Shelnutt, J. A.; Medforth, C. J.; Berber, M. D.; Barkigia, K. M.; Smith, K. M. *J. Am. Chem. Soc.* **1991**, *113*, 4077−4087. (c) Medforth, C. J.; Senge, M. O.; Smith, K. M.; Sparks, L. D.; Shelnutt, J. A. *J. Am. Chem. Soc.* **1992**, *114*, 9859−9869.
(32) Rankin, J. G. Ph.D. Dissertation, University of Houston, 1993.
(33) Barkigia,, K. M.; Renner, M. W.; Furenlid, L. R.; Medforth, C. J., Smith, K. M.; Fajer, J. *J. Am. Chem. Soc.* **1993**, *115*, 3627−3635.

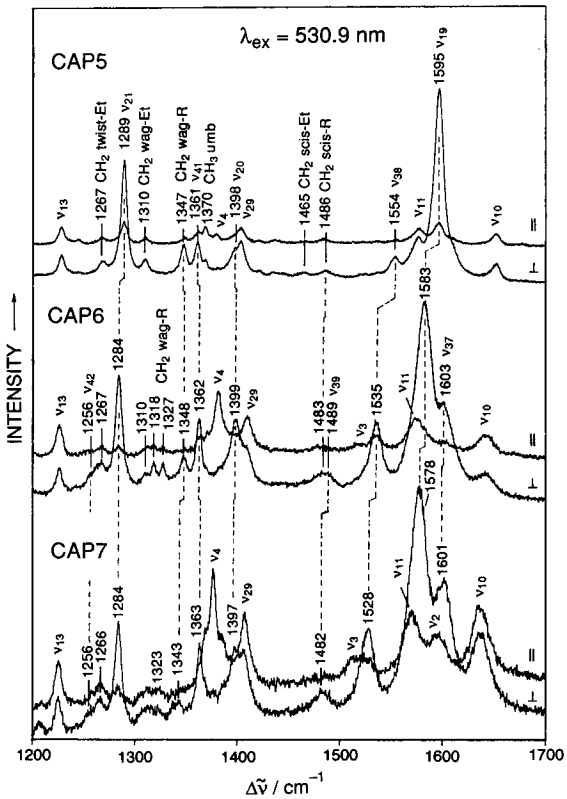

Figure 4. Same as Figure 3, but with 530.9-nm excitation and 2-cm^{-1} slit widths. Anomalously polarized (A_{2g}) bands are correlated.

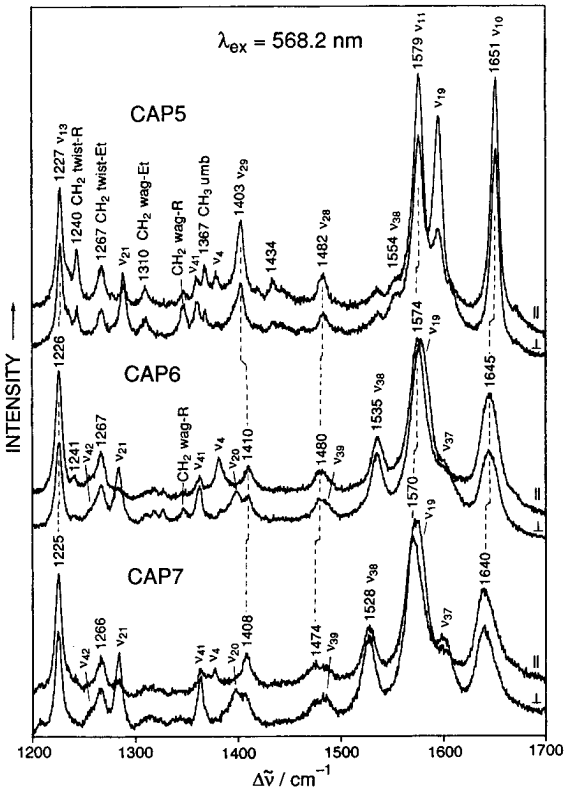

Figure 5. Same as Figure 3, but with 568.2-nm excitation and 2-cm^{-1} slit widths. Depolarized (B_{1g}, B_{2g}) bands are correlated.

the high frequency NiCAP5 modes are lower in frequency (up to 9 cm^{-1} for ν_{21}) than the corresponding modes of NiEtio-II, except for the ν_3 stretch at 1535 cm^{-1} which is 13 cm^{-1} higher than that of NiEtio-II (1522 cm^{-1}) (Table 3). In fact, the 1535-cm^{-1} frequency of the ν_3 mode appears to be unique to the CAP5 structure as no other petroporphyrins studied so far show such a high frequency for this mode, which typically occurs at 1510−1520 cm^{-1} in alkyl porphyrins.[18]

Also unique for NiCAP5 only is the oxidation state marker mode, ν_4, which in alkyl porphyrins usually gives rise to the strongest band near 1380 cm^{-1} in the Soret-excited spectrum. Indeed, Figure 3 shows that the ν_4 mode can readily be identified for NiCAP6 and NiCAP7 with the very strong polarized bands at 1381 and 1376 cm^{-1}, respectively, but the NiCAP5 spectrum in this region becomes unusually complicated and shows several dramatically weakened polarized bands between 1350 and 1380 cm^{-1}. In this case, unambiguous identification of the ν_4 band must await testing for sensitivity to isotopic substitution of the pyrrole nitrogens.[18b] However, it is interesting to note that chlorophyll *a* also shows a marked decrease in the intensity and splitting for ν_4 relative to other bands.[34] This implies that multiple components and decreased intensity of the ν_4 mode may be a characteristic feature of the petroporphyrin structure bearing a five-membered exocyclic ring.

Careful examination of Figures 3−5 reveals that the high-frequency in-plane skeletal bands are also influenced by the size of the *meso*,*β*-alkano ring. In particular, the structure-sensitive modes,[35] ν_2, ν_3, ν_{10}, ν_{11}, ν_{19}, and ν_{28}, are all systematically downshifted in frequency with increasing size of the exocyclic ring. The ν_3 mode shifts the most, −24 cm^{-1} between NiCAP5 and NiCAP7, followed by the ν_{19} (−17 cm^{-1}) and ν_{10} (−11 cm^{-1}) modes. These modes, which primarily involve stretching of the $C_\alpha-C_m$ bonds (see Table 3), have traditionally been used as indicators of the porphyrin core expansion (core size marker bands), because they consistently decrease in frequency when the size of the porphyrin cavity increases.[18a] Simple linear empirical relationships have been established for metallo-OEP, between frequencies of ν_3, ν_{10}, and ν_{19} and a porphyrin core size.[36] Using those parameters,[36] an increase in core size would be ∼0.015 Å going from NiCAP5 to NiCAP6 and from NiCAP6 to NiCAP7 based on the respective ν_{10} and ν_{19} frequencies but ∼0.04 Å based on ν_3 for NiCAP5 to NiCAP6 and only ∼0.01 Å for NiCAP6 to NiCAP7. Shelnutt and co-workers[30,37] noted considerable downshifts in these same bands for a series of highly distorted nickel porphyrins, which they attributed to the nonplanarity of the macrocycle resulting from the steric crowding induced by the substituent groups. Both ruffling and saddle distortions were reported. They did state that for nonplanar porphyrins the relationship between core-size marker band Raman shifts and actual core size did not hold for highly distorted macrocycles.[37c] Because there is no reason to expect that the porphyrin cavity should increase in NiCAPs merely because of different lengths of the bridging alkano substituents, the substantial frequency depressions of the structure-sensitive bands going from NiCAP5 to NiCAP6 to NiCAP7 must rather be due to nonplanar distortions. The distortion from planarity caused by increased size of the *meso*,*β*-alkano chain results in decreased π-conjuga-

(34) Lutz, M.; Robert B. In *Biological Applications of Raman Spectroscopy*; Spiro, T. G., Ed.; Wiley: New York, 1988; Vol. 3, pp 347−411.
(35) Spaulding, L. D.; Chang, C. C.; Yu, N.-T.; Felton R. H. *J. Am. Chem. Soc.* **1975**, *97*, 2517−2525.
(36) Prendergast, K.; Spiro, T. G. *J. Am. Chem. Soc.* **1992**, *114*, 3793−3801.
(37) (a) Shelnutt, J. A.; Majumder, S. A.; Sparks, L. D.; Hobbs, J. D.; Medforth, C. J.; Senge, M. O.; Smith, K. M.; Miura, M.; Luo, L.; Quirke, J. M. E. *J. Raman Spectrosc.* **1992**, *23*, 523−529. (b) Sparks, L. D.; Medforth, C. J.; Park, M. S.; Chamberlain, J. R.; Ondrias, M. R.; Senge, M. O.; Smith, K. M.; Shelnutt, J. A. *J. Am. Chem. Soc.* **1993**, *115*, 581−592. (c) Stichtermath, A.; Schweitzer-Stenner, R.; Dreybrodt, W.; Mak, R. S.; Li, X.-Y.; Sparks, L. D.; Shelnutt, J. A.; Medforth, C. A.; Smith, K. M. *J. Phys. Chem.* **1993**, *97*, 3701−3708. (d) Sparks, L. D.; Chamberlain, J. R.; Hsu, P.; Ondrias, M. R.; Swanson, B. A.; Ortiz de Montellano, P. R.; Shelnutt, J. A. *Inorg. Chem.* **1993**, *32*, 3153−3161.

Table 3. In-Plane Skeletal RR Frequencies (cm^{-1}) and Local Mode Assignments for Ni(II) Complexes of Etio-II, CAP5, CAP6, and CAP7[a]

			RR frequencies			
sym	ν_i	description[b]	Etio-II	CAP5	CAP6	CAP7
A_{1g}	ν_2	$\nu(C_\beta C_\beta)$	1607	1607	1603	1596
	ν_3	$\nu(C_\alpha C_m)_{sym}$	1522	1535	1515	1511
	ν_4	ν(Pyr half-ring)$_{sym}$	1381	1379	1381	1376
	ν_5	$\nu(C_\beta C_1)_{sym}$	1136	1129/1138	1135/1146	1133/1137
	ν_6	ν(Pyr breathing)	815	818	818	820
	ν_7	δ(Pyr def)$_{sym}$	676	705	704	707
	ν_8	$\delta(C_\beta C_1)_{sym}$	342	342/354	342/325	344/361
	ν_9	ν(NiN)	260	272/265	276/272	280/255
B_{1g}	ν_{10}	$\nu(C_\alpha C_m)_{asym}$	1655	1651	1645	1640
	ν_{11}	$\nu(C_\beta C_\beta)$	1579	1576	1574	1570
	ν_{12}	ν(Pyr half-ring)$_{sym}$	1384[c]		1383sh	1384
	ν_{13}	$\delta(C_m H)$	1226	1227	1226	1225
	ν_{14}	$\nu(C_\beta C_1)_{sym}$	1129	1143	1146	1146
	ν_{15}	ν(Pyr breathing)	751	757	758	756
	ν_{16}	δ(Pyr def)$_{sym}$	753		753	
	ν_{17}	$\delta(C_\beta C_1)_{sym}$	293			
	ν_{18}	ν(NiN)	170		168	
A_{2g}	ν_{19}	$\nu(C_\alpha C_m)_{asym}$	1603	1595	1583	1578
	ν_{20}	ν(Pyr quarter-ring)	1398	1398	1399	1397
	ν_{21}	$\delta(C_m H)$	1305	1284	1284	1284
	ν_{22}	ν(Pyr half-ring)$_{asym}$	1120	1121	1117	1118
	ν_{23}	$\nu(C_\beta C_1)_{asym}$	1059	1059	1058	1060
	ν_{24}	δ(Pyr def)$_{asym}$	591	584	593	
	ν_{25}	δ(Pyr rot)	553	555	558	557
B_{2g}	ν_{28}	$\nu(C_\alpha C_m)_{sym}$	1484	1482	1481	1474
	ν_{29}	ν(Pyr quarter-ring)	1409	1403	1410	1408
	ν_{30}	ν(Pyr half-ring)$_{asym}$	1160	1155	1162	1157
	ν_{31}	$\nu(C_\beta C_1)_{asym}$	1010	1001	1001	998
	ν_{32}	δ(Pyr def)$_{asym}$	948	942	931	933
	ν_{33}	δ(Pyr rot)	490	482	486	486
	ν_{34}	$\delta(C_\beta C_1)_{asym}$	197	206	199	201
E_u	ν_{37}	$\nu(C_\beta C_\beta)$	[1602][d]		1603	1601
	ν_{38}	$\nu(C_\alpha C_m)_{asym}$	1570	1554	1535	1528
	ν_{39}	$\nu(C_\alpha C_m)_{sym}$	1496		1489	1482
	ν_{40}	ν(Pyr quarter-ring)	1393			
	ν_{41}	ν(Pyr half-ring)$_{sym}$	[1363]	1361	1362	1363
	ν_{42}	$\delta(C_m H)$	1230		1256	1256
	ν_{43}	ν(Pyr half-ring)$_{asym}$	1147			
	ν_{44}	$\nu(C_\beta C_1)_{sym}$	1125		1126	1128

[a] Mode frequencies from CS_2 solution RR spectra at room temperature. [b] See refs 26 and 27 for local coordinate definitions. [c] This value from KCl pellet FT-Raman spectrum (1068-nm excitation) of NiEtio-I;[42] not observed in natural abundance NiEtios with visible excitations, but seen at ~1324 cm^{-1} in *meso*-d_4 isotopomers.[19,32] [d] These E_u-mode frequencies from KBr pellet IR spectra of NiEtio-I. Values in brackets are calculated frequencies, not observed.[42]

tion within the porphyrin macrocycles, hence weakening the skeletal bonds and lowering the Raman frequencies. This decrease in frequency of the structure-sensitive bands is common to all nonplanar porphyrins studied so far.[30,33,37,38] That the porphyrin macrocycle deviates more from planarity in NiCAP6,7 than NiCAP5, rather than expanding, is further evidenced in the significantly increased half-band width of the structure-sensitive RR bands (compare, e.g., ν_{10} modes in Figure 5).

X-ray crystallographic data are not available for any of the NiCAPs studied by RR spectroscopy in this work. However, the X-ray structure of nickel(II) deoxophylloerythrin methyl ester (NiDPE) with a five-membered exocycle has been reported.[39] This compound is closely related to the petroporphyrin DPEP (having 13,15-ethano chain) but still retains the propionic acid side chain of chlorophyll *a* at position 17. The triclinic crystalline NiDPE is slightly ruffled.[39] Bond lengths and angles for most of the molecule are within errors of measurement to the orthorhombic NiEtio-III.[32] In contrast, bond angles of NiDPE involving pyrrole C and the exocyclic ring deviate significantly. For example, the $C_\alpha-C_m-C_\alpha$ angle in NiEtio-III is ~125° and the $C_\beta-C_\alpha-C_m$ angle is ~124°, whereas in NiDPE the corresponding angles where the exocyclic ring is attached are 121 and 114°, respectively (rms of the bond angles is less than 1°). Porphyrin skeletal vibrations involving stretching of bonds making up either of these angles are expected to be perturbed; these structure differences, if present in NiCAP5, may explain the significant upshift of ν_3 which is primarily $\nu(C_\alpha C_m)$ in character. Further, the $C_\beta-C_\beta-C_1$ and $C_\beta-C_1-C_2$ angles are also distorted, which should affect peripheral substituent modes. These are discussed below.

b. New Anomalously Polarized Bands. It is also interesting to note that NiCAPs are unique in that they give rise to an increased number of anomalously polarized bands in the RR spectra as compared to NiEtios and NiTHBPs, which are best seen with 530.9-nm excitation in Figure 4. Several of these in the 1340−1365- and 1485-cm^{-1} regions can be identified with the CH_2 wagging and scissoring motions,[40] respectively, of the *meso*,β-alkano ring methylene groups. While similar modes are activated in NiEtios and NiTHBPs spectra, those modes appear stronger as their p and dp combinations rather than ap.[19−21] Why this is the case is not clear at this moment. In addition, both the NiCAP6 and NiCAP7 show at least two more ap bands (~1320 cm^{-1}) in the CH_2 wagging region, consistent

(38) (a) Czernuszewicz, R. S.; Li, X.-Y.; Spiro, T. G. *J. Am. Chem. Soc.* **1989**, *111*, 7024−7031. (b) Li, X.-Y.; Czernuszewicz, R. S.; Kincaid, J. R.; Spiro, T. G. *J. Am. Chem. Soc.* **1989**, *111*, 7012−7023.
(39) Petterson, R. C. *J. Am. Chem. Soc.* **1971**, *93*, 5629−5632.
(40) Colthup, N. B.; Daly, L. H.; Wiberly, S. E. *Introduction to Infrared and Raman Spectroscopy*, 3rd ed.; Academic Press: Boston, MA, 1990.

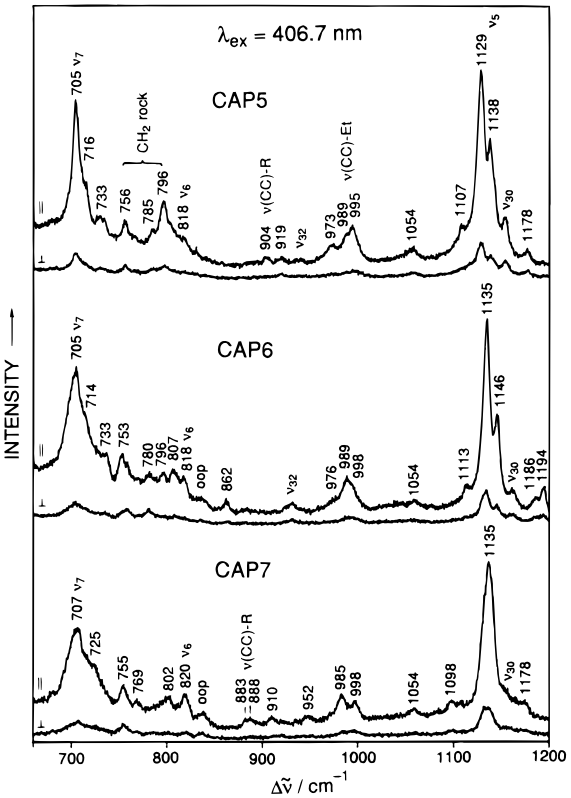

Figure 6. RR spectra in CS_2 of Ni(II) complexes of CAP5 (top), CAP6 (middle), and CAP7 (bottom), obtained with 406.7-nm excitation in the 600−1200-cm^{-1} region. Solvent bands marked with asterisks. Conditions: backscattering from spinning NMR tube; 150-mW laser power; 3-cm^{-1} slit widths; average of three scans, each scan with 1-s integration time per point at 0.5-cm^{-1} increments.

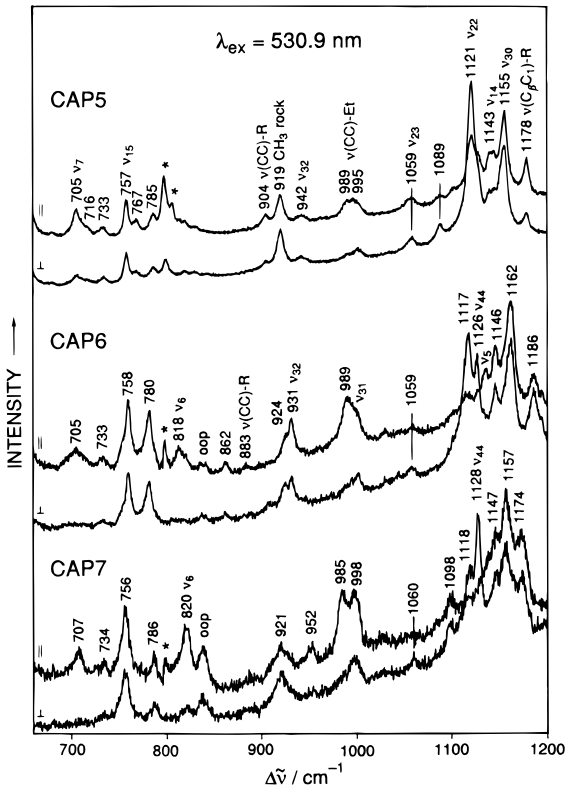

Figure 7. Same as Figure 6, but with 530.9-nm excitation.

with the increased number of methylene groups relative to those in NiCAP5, albeit these bands in NiCAP7 are somewhat broad and poorly resolved (Figure 4).

The most dramatic difference between the RR spectra of NiCAPs, NiEtios and NiTHBPs, however, is the strong appearance of new ap bands in NiCAPs above 1500 cm^{-1} (Figure 5). In the NiCAP5 spectrum (top), one of these bands is located at 1554 cm^{-1} which both significantly downshifts in frequency and increases in intensity with elongated cycloalkano substituents. The second ap band in this region appears only in NiCAP6 (middle) and NiCAP7 (bottom), at ∼1600 cm^{-1}, again the NiCAP7 band (1603 cm^{-1}) being clearly stronger than that of NiCAP6 (1601 cm^{-1}). A comparison of the three spectra reveals that these spectral changes are associated with a concomitant marked decrease in the intensity of the dominant porphyrin skeletal modes ν_{21} ($\delta(C_mH)$) and ν_{19} ($\nu(C_\alpha C_m)_{sym}$), on going from NiCAP5 to NiCAP6 to NiCAP7 (relative, for example, to ν_4, ν_{13}, and ν_{29}). The ν_{21} and ν_{19} modes are found at 1289 and 1595 cm^{-1}, respectively, for NiCAP5 and are 5−8 cm^{-1} lower in frequency than their counterparts in NiEtio-II (Table 2). The ring size has a mixed effect on the frequency of ν_{21}; there is no change between NiCAP6 and NiCAP7 and a 5-cm^{-1} downshift going from NiCAP5 to NiCAP6. As discussed above, the ν_{19} mode is influenced significantly, shifting −17 cm^{-1} between NiCAP5 and NiCAP7 due to nonplanar distortions of the porphyrin macrocycle. Inasmuch as the bands arising from the ν_{21} and ν_{19} vibrations are also relatively weaker, these 1520−1555- and ∼1600-cm^{-1} ap bands in NiCAPs most likely gain their intensities at the expense of ν_{21} and ν_{19} by a redistribution of vibronic coupling that gives rise to the Q_1 absorption sideband.

As for the assignment, these two new ap bands most likely originate from the IR-active skeletal modes (E_u in D_{4h} symmetry) because of symmetry lowering and inversion center loss of the porphyrin macrocycle due to asymmetric nonplanar distortion by the exocyclic ring. A loss of the center of symmetry, seen in crystal structures of NiDPE and (VO)DPEP, would lead to RR activation of E_u modes which could become anomalously polarized under resonance excitation conditions[41] via vibrational mixing with A_{2g} skeletal modes. The two possible candidates are the ν_{37} (for the 1601-cm^{-1} band) and ν_{38} (for the 1520−1550-cm^{-1} band) skeletal modes involving predominantly $\nu(C_\beta C_\beta)$ and $\nu(C_\alpha C_m)_{asym}$ stretches, respectively, because these modes are observed (IR spectra) and calculated near 1600 (ν_{37}) and 1570 cm^{-1} (ν_{38}) for NiEtio-I.[42] Several other candidates for the E_u-derived vibrations in the high-frequency region are the ap bands at 1489, 1362, and 1256 cm^{-1} in NiCAP6 (Figures 4 and 5), assignable to $\nu(C_\alpha C_m)_{asym}$ (ν_{39}), ν(Pyr half-ring)$_{sym}$ (ν_{41}), and $\delta(C_mH)$ (ν_{42}), respectively (Table 3), because (1) these bands are either absent or very weak in NiCAP5, (2) they occur even more strongly at 1482, 1363, and 1256 cm^{-1} in the apparently more distorted NiCAP7, and (3) these frequencies correspond well to the NiEtio-I IR peaks at 1496 (ν_{39}), 1363 (ν_{41}) (calculated), and 1230 cm^{-1} (ν_{42}).[42]

c. The 650−1200-cm^{-1} Region. The midrange (650−1200 cm^{-1}) RR spectra of the three NiCAPs obtained with the 406.7-, 530.9-, and 568.2-nm excitation wavelengths are presented in Figures 6−8, respectively. Several noteworthy differences occur in this region which allow one to differentiate NiCAPs from other petroporphyrins characterized thus far, and to distinguish each of the NiCAPs. The strongest dp band in the mid-range of the 568.2-nm-excited spectra of NiEtios and NiTHBPs is found near 750 cm^{-1}, assignable to the B_{1g} pyrrole breathing mode ν_{15}.[19−21] The corresponding band in NiCAPs shifts up to ∼757 cm^{-1} and is only about one half as intense relative to other skeletal vibrations (Figure 8). Cycloalkano ring size seems to have little effect, less than ±1 cm^{-1}, on the position of this

(41) Clark, R. J. H.; Stewart, B. *Struct. Bonding (Berlin)* **1979**, *36*, 1−80.
(42) Hu, S.; Mukherjee, A.; Piffat-Mason, C.; Mak, R. S. W.; Li, X. -Y.; Spiro, T. G. To be submitted for publication.

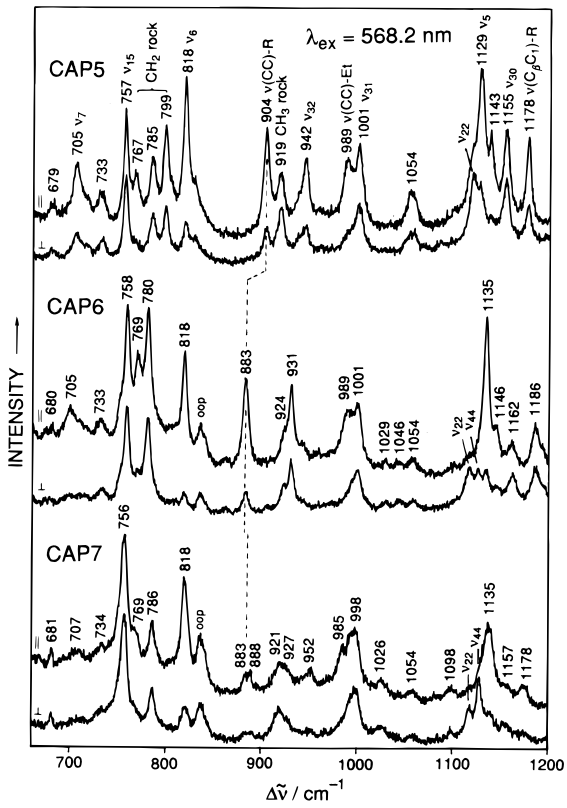

Figure 8. Same as Figure 6, but with 568.2-nm excitation.

mode; thus, this may be a general diagnostic feature when a porphyrin is bearing any exocycle on the *meso* and β-carbons. An even more characteristic vibrational feature of the cycloalkano structure is the polarized skeletal mode ν_7 found in all three NiCAPs at ~705 cm^{-1} (seen best in Figure 6 with 406.7-nm excitation), assignable to the A_{1g} deformation mode of the pyrrole rings, ν(Pyr def), because its counterparts in other petroporphyrins occur at drastically lower frequencies, ~675 cm^{-1} in NiEtios[19,20] and ~672 cm^{-1} in NiTHBPs.[21] This mode is effected by exocyclic ring size; namely, it is intense and sharp in NiCAP5 but both markedly broadens and loses intensity in NiCAP6 and NiCAP7.

Further careful examination of the 660−1200-cm^{-1} region reveals characteristic patterns of bands which permit easy differentiation of the three nickel CAPs. In the 1100−1200-cm^{-1} region, especially in the Soret-excited spectra (Figure 6), there are two strong polarized bands near 1135 cm^{-1} which are attributed to the A_{1g} component of the predominantly $\nu(C_\beta C_1)$ mode, ν_5. These bands are well resolved for NiCAP5 (Figure 6, top, 1129 and 1138 cm^{-1}) and NiCAP6 (middle, 1135 and 1146 cm^{-1}), but collapse into a broad asymmetric peak centered near 1135 cm^{-1} in NiCAP7 (bottom). [In the perpendicular spectrum, the ~1135-cm^{-1} peak appears to split into two components at 1133 and 1137 cm^{-1}.] A similar splitting of ν_5 was observed for NiTHBPs where the higher (~1143 cm^{-1}) frequency component was assigned to $\nu_5(C_\beta C_1)$-Me involving methyl peripheral substituents and the lower one (1132 cm^{-1}) involving ethyl groups, $\nu_5(C_\beta C_1)$-Et.[21] Thus, on the basis of the similarity in frequencies, analogous assignments are made for the NiCAPs (Table 2).

Additional clear differences between the 1100−1200-cm^{-1} RR bands of the three NiCAPs are evident in the 568.2-nm-excited spectra shown in Figure 8. The most significant difference is that, besides the ν_5 bands described above, NiCAP5 shows two strong bands in this region at 1155 (dp) and 1178 cm^{-1} (mostly p) which are either very weak or absent in NiCAP6 and NiCAP7 spectra. The 1155-cm^{-1} dp band is identified with the asymmetric pyrrole half-ring stretch, ν_{30} (B_{1g}).[26] This mode can be weakly seen for NiCAP6 at higher frequency, 1162 cm^{-1}, while in the NiCAP7, it is essentially gone (only a very weak bump occurs near 1157 cm^{-1}). Interestingly however, the ν_{30} mode appears to regain intensity when the NiCAP6 and NiCAP7 molecules are excited with a 530.9-nm laser line (Figure 7). With this excitation all three NiCAPs show well-defined bands in the 1160-cm^{-1} region of nearly equal intensities, at 1155 (NiCAP5), 1162 (NiCAP6), and 1157 cm^{-1} (NiCAP7), the perpendicular scattering components of which are equal or exceed the parallel ones ($\rho \geq 1$). This dispersion of the depolarization ratio further indicates that the symmetry of the basic porphyrin ring is lower than D_{4h} in NiCAPs as a consequence of nonplanar distortion which is reflected in the downshifted structure-sensitive skeletal vibrational modes discussed in the previous section. A similar dispersion in ρ is seen for the 1186-cm^{-1} band which shows up only in the NiCAP6 spectra (Figures 7 and 8). This feature appears to be characteristic of the NiCAP6 vibrational spectrum as well. The origin of the 1186-cm^{-1} band is not clear. However, it is a good candidate for the B_{1g} mode ν_{14} involving the exocyclic ring coordinates, because this frequency is close to that of the ν_{14} mode of NiTBuP (TBuP = tetra-β,β-butanoporphyrin), 1165 cm^{-1}.[21] A dp band at 1174 cm^{-1} in the 530.9-nm-excited spectrum of NiCAP7 may arise from a similar vibration, and thus shows exocycle ring size dependence.

The strong polarized band found at 1178 cm^{-1} in NiCAP5 spectra, particularly with 568. 2-nm excitation (Figure 8), most likely arises from the same vibrational mode as those near 1175 cm^{-1} of NiTHBPs and NiTBuP which have been ascribed to $\nu_5(C_\beta C_1)$-R (R = exocyclic ring).[21] It totally disappears in the NiCAP6 spectrum and loses most of its intensity in the NiCAP7 spectrum, suggesting subtle structural variation near pyrroles bearing the exocycle ring. Although not present in the 568.2-nm-excited spectrum of NiCAP6, this mode may possibly be detected in resonance with the Soret-band, because the 406.7-nm excitation exposes a weak polarized doublet at higher frequency (1187, 1194 cm^{-1}) which is absent in the other two NiCAPs (Figure 6).

Finally, the A_{2g} $\nu(\text{Pyr half-ring})_{asym}$ mode, ν_{22}, is assigned to the ap band at 1121 cm^{-1} for NiCAP5 (Figure 7, 530.9-nm excitation). This band clearly splits into two ap bands for NiCAP6 (1117 and 1126 cm^{-1}) and NiCAP7 (1118 and 1128 cm^{-1}), most likely due to RR activation of the E_u $\nu(C_\beta C_1)$ stretch (IR-active skeletal mode ν_{44}) which is also expected to vibrate with frequency in this region.[26,42] Although the frequencies for this pair of bands are similar for NiCAP6 and NiCAP7, the relative intensities are very different, with the lower frequency band (ν_{22}) being more intense in NiCAP6 but with the higher frequency one (ν_{44}) being more intense in NiCAP7. Thus, the characteristic frequency and intensity pattern of the ν_{22} and ν_{44} RR modes allows easy identification of the three NiCAPs.

3. Exocyclic and Alkyl Substituent Modes. As discussed above, the 650−1200-cm^{-1} porphyrin skeletal modes in the RR spectrum (especially with 568.2-nm excitation wavelength) can be used to identify the presence of a cycloalkano exocycle as well as determine its ring size to some extent. However, this region is also expected to contain useful bands due to vibrational modes associated with alkyl and cycloalkyl peripheral substituents. For the NiTHBPs, the 1050−1100-cm^{-1} bands attributed to the β,β-butano exocycle C−C stretching modes proved to be the most useful marker bands of tetrahydrobenzoporphyrin structure in this region.[21] Because variations in cycloalkano ring size in NiCAPs are expected to have an effect on the vibrational pattern of the the ν(CC)-R stretches, these modes, along with the terminal alkyl stretching and deformation modes,

should provide characteristic patterns of bands making up each compound's unique "fingerprint". Only weak bands are found in the spectra of all three NiCAPs in the region where ν(CC)-R modes of NiTHBP are found. Although weak, these bands do differ among the samples of NiCAP5 through NiCAP7. Thus, as can be seen in Figure 8, a single dp band occurs at 1054 cm^{-1} in NiCAP5, which appears to split into three weak dp bands at 1029, 1046, and 1054 cm^{-1} in NiCAP6 and several weak bands spanning the 1025−1090-cm^{-1} range in NiCAP7. If not all, at least some of them may involve stretching of the exocyclic C−C bonds in keeping with the 1050−1100-cm^{-1} bands of NiTHBPs whose assignments are more secure.[21]

Significantly, however, a strong polarized band is found at 904 cm^{-1} in the NiCAP5 spectrum with Q-band excitation (568.2 nm) in Figure 8 (top) which does not show up in either NiEtios or NiTHBPs. This characteristic feature correlates with a similar band at 883 cm^{-1} in NiCAP6 and a markedly weaker doublet, 883/888 cm^{-1}, in NiCAP7. This ∼900-cm^{-1} band of NiCAPs may arise from stretching of the outer single C−C bonds of the *meso*,*β*-alkano ring, because of similar frequencies observed for cycloalkenes which all show strong polarized Raman bands in the 800−900 cm^{-1} region assignable to the symmetric C−C stretch.[43] Its dependence on the size of the exocycle ring lends additional support for this assignment. Also unique in this region is the feature at 919 cm^{-1} in the NiCAP5 spectra with 530.9- and 568.2-nm excitations (Figures 7 and 8). The assignment of this band, which appears to dramatically lose intensity with increasing exocycle ring size (only shoulders can be seen at similar frequencies for NiCAP6 and NiCAP7) is uncertain; however, a CH_3 rocking mode has been assigned to a weak ap band in this region for NiOEP[26] and NiEtios.[19,42]

A comparison of the three NiCAPs spectra in Figure 8 also reveals a cluster of bands over the 750−825-cm^{-1} range, each porphyrin displaying a very different vibrational pattern. The modes expected in this region encompass ν_{15} (dp), ν_{16} (dp) and ν_6 (p) skeletal and CH_2 rocking alkyl substituent vibrations. The ν_{15} band at 757 cm^{-1} has already been discussed in the previous section. The only strong polarized band in this region is seen near 819 cm^{-1} for all three NiCAPs, and is therefore ascribed to ν_6, a totally symmetric pyrrole breathing mode (Table 3). The frequency of this mode is not perturbed very much by the size of the *meso*,*β*-alkano ring; however, it is significantly upshifted (10−35 cm^{-1}) with respect to other alkyl porphyrins.[19−21,26]

More dramatic differences between NiCAP5, NiCAP6, and NiCAP7 are seen in the multiple bands located in between the ν_{15} and ν_6 bands, where the methylene rocking vibrations are expected to occur. Two such bands at 770 (p) and 781 cm^{-1} (dp) have been identified in NiOEP spectra as CH_2 rocking modes of the ethyl substituents, also with 568.2-nm excitation, on the basis of methylene-d_{16} shifts and normal mode calculations.[26] The CH_2 rocking modes were also revealed in this region for NiEtios by examining the RR spectra of NiEtio-III-d_{20} isotopomer.[19] NiCAP5 shows three bands in this region at 767 (p), 785 (dp), and 799 cm^{-1} (dp), whereas NiCAP6 and NiCAP7 each show only two at 769 (p), 780 (dp) and 769 (p), 786 cm^{-1} (dp), respectively. Not only are the positions of these bands influenced by the exocycle ring size, but their intensities vary dramatically as well, as demonstrated by Figure 8. Of particular interest is that the ∼780 cm^{-1} dp band in the NiCAPs is strikingly strong, whereas in other petroporphyrins it is weak (NiTHBPs, ∼772 cm^{-1}) or absent (NiEtios).[19−21] Because it changes with ring size (785/799 cm^{-1} for NiCAP5, 780 cm^{-1} for NiCAP6, and 786 cm^{-1} for NiCAP7) and substituent groups at tetrapyrrolic C-13 and/or cycloalkano ring itself,[32] it is likely that the exocyclic ring methylenes are involved. Precise analysis of the bands in this extremely useful region must await the additional data from selectively isotopically labeled molecules and normal coordinate analysis calculations.

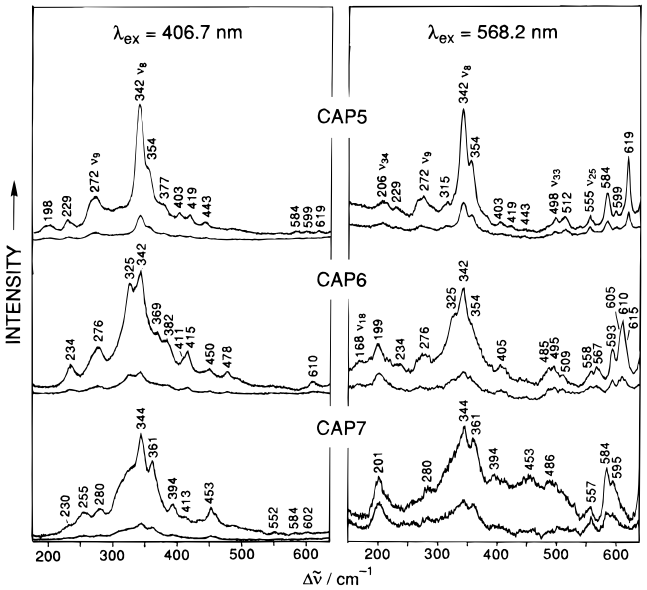

Figure 9. Low-frequency RR spectra of Ni(II) complexes of CAP5 (top), CAP6 (middle), and CAP7 (bottom) (∼1 mM) in CS_2, obtained with 406.7- (left) and 568.2-nm (right) excitations, respectively. Conditions for all spectra: backscattering from spinning NMR tube; 150-mW laser power; 3-cm^{-1} slit widths; three scans, each with 1-s integration time per point at 0.5- cm^{-1} increments.

The C−C stretching modes of ethyl and methyl groups are expected in the 1000-cm^{-1} region, and two moderately strong bands are found there for each of the NiCAPs with 568.2-nm excitation (Figure 8), a p band near 987 cm^{-1} and a dp one near 1000 cm^{-1} (a ν_{31} skeletal mode, also expected at ∼1000 cm^{-1}, may contribute some intensity to the dp band). The vibrational pattern of these two bands is reminiscent of the 980−1010-cm^{-1} features of NiEtio-II in that the dp band is higher in frequency than the p band.[20] This is perhaps not surprising because the pyrroles bearing only methyl and ethyl groups in the two porphyrin types have the same C_2 local symmetry (Figure 1). Indeed, the *meso*,*β*-alkano ring has essentially no effect on these bands, suggesting that they involve in-phase (p mode) and out-of-phase (dp mode) combinations of the C−C coordinates of the ethyls specifically localized on the neighboring pyrroles.

A number of bands in the high frequency region (1300−1500 cm^{-1}) have been assigned to CH_2 scissoring and wagging motions either due to the ethyl substituents or ring methylenes (Table 2) based on similar bands in nickel Etios[19] and OEP.[26] The CH_3 deformation modes of either the methyl or ethyl groups are assigned to ap and dp bands around 1360 cm^{-1}. A polarized band at 1240 cm^{-1} is assigned to CH_2 twisting motion of the exocyclic ring based on the presence of a similar band in NiTBuP which has no ethyl groups.[21]

Generally, the low frequency (<650 cm^{-1}) RR spectra of metalloalkylporphyrins are dominated by the strongly coupled C_β−C_1 bending/metal−pyrrole breathing mode, ν_8 (A_{1g}), which gives rise to a polarized band in the 340−400-cm^{-1} region.[18,26] As might be expected, the nickel cycloalkanoporphyrins are no exception, and Figure 9, which compares the CS_2 solution spectra of NiCAP5, NiCAP6, and NiCAP7 obtained with Soret- (406.7 nm, left) and Q-band (568.2 nm, right) excitations, reveals very intense polarized bands in the 340-cm^{-1} region

(43) (a) Neto, N.; Di Lauro, C.; Castellucci, E.; Califano, S. *Spectrochim. Acta* **1967**, *23A*, 1763−1774. (b) (a) Neto, N.; Di Lauro, C.; Califano, S. *Spectrochim. Acta* **1970**, *26A*, 1489−1509.

which can no doubt be assigned to ν_8. More importantly, these bands are also strongly influenced by the size of the exocycle, further aiding in the quest of developing RR spectroscopy as a probe of petroporphyrin structure. Thus, NiCAP5 displays a prominent polarized band at 342 cm^{-1} with a shoulder at 354 cm^{-1}, NiCAP6 has two such bands at 342 and 325 cm^{-1}, and NiCAP7 displays a very broad polarized envelope between 300−375 cm^{-1} with only visible peaks at 344 and 361 cm^{-1}. A weaker polarized band at 272 cm^{-1} in NiCAP5 arises from the in-plane skeletal mode, ν_9, the only other totally symmetric skeletal mode (mainly Ni−pyrrole breathing) expected below 400 cm^{-1} (Table 3). It also varies with the exocycle size, shifting up to 276 cm^{-1} in NiCAP6 and splitting into a 255/280-cm^{-1} doublet in NiCAP7.

This splitting and broadening of ν_8 and ν_9 in solution, especially for NiCAP7, probably reflects several coexisting conformers which may differ in orientation of the ethyl substituents relative to the exocycle. The splitting of ν_8 and ν_9 was observed in solution RR spectra for NiOEP[26] and (VO)-Etio-I,[19] which was attributed to the presence of different ethyl orientational conformers. The exocycle itself may adopt different conformations in solution as well, because cycloheptene, in liquid, exists in equilibrium between the chair and boat conformations.[43b] The kinematics of the various possible NiCAP conformers remain to be investigated.

Further examination of the NiCAP low-frequency spectra reveals a cluster of polarized bands in the 580−620-cm^{-1} region which have not been observed in other petroporphyrins. Consequently, these new characteristic bands can be ascribed to the deformation modes of the saturated carbon exocycle substituent which may serve as signatures for the NiCAPs. They are most apparent in the Q-band-excited spectra with 568.2-nm laser line (Figure 9, right), each NiCAP showing a distinctive vibrational signature depending upon the cycloalkano ring size. NiCAP5 displays two sharp polarized bands at 619 and 584 cm^{-1}, whereas NiCAP6 has a broad feature centered about 610 cm^{-1} containing three overlapping peaks (605, 610, 615 cm^{-1}) and a smaller single band at 593 cm^{-1}. It appears that the higher frequency bands (>600 cm^{-1}) in this region downshift into the 584/595-cm^{-1} doublet in the NiCAP7 spectrum.

Conclusions

The Soret- and Q-band excited resonance Raman spectra of the nickel cycloalkanoporphyrins are richly populated with numerous vibrational modes that can be used to obtain structural information about *meso,β*-strapped petroporphyrins. Generally, for metalloalkylporphyrins the most useful Raman modes are the structure-sensitive modes, ν_2, ν_3, ν_{10}, ν_{11}, ν_{19}, and ν_{28}, and we have demonstrated that these modes are very informative when comparing NiCAPs to the other petroporphyrins (NiEtios and NiTHBPs). For example, these modes shifted to lower frequencies for NiCAP5 relative to NiEtios and NiTHBPs. These downshifts are a result of the weakening of skeletal bonds as a consequence of slightly disrupted π-conjugation in the porphyrin macrocycle upon strapping the β and *meso* carbons with an alkano chain. The NiCAP5 also shows the ν_3 mode (ν-$(C_\alpha C_m)_{sym}$) at unusually high frequency (1535 cm^{-1}) and multiple bands in the ν_4 mode (ν(Pyr half-ring)$_{sym}$) region (1360−1385 cm^{-1}) with dramatically diminished intensity, which may serve as signatures for the NiCAP5 structure.

The high frequency structure-sensitive modes are all systematically downshifted in frequency by as much as 25 cm^{-1} with increasing size of the cycloalkano ring (Figure 10). This is attributed to the increasing nonplanarity of the porphyrin macrocycle distorted by the steric crowding of the exocycle. Consistent with this, there is a progressive bathochromic shift in the Soret- and Q-bands in the UV−visible absorption spectra with increasing exocycle size, and new anomalously polarized peaks appear upon Q-band excitation in the RR spectra which can be assigned to porphyrin E_u skeletal modes activated by the lower symmetry of the nonplanar NiCAPs.

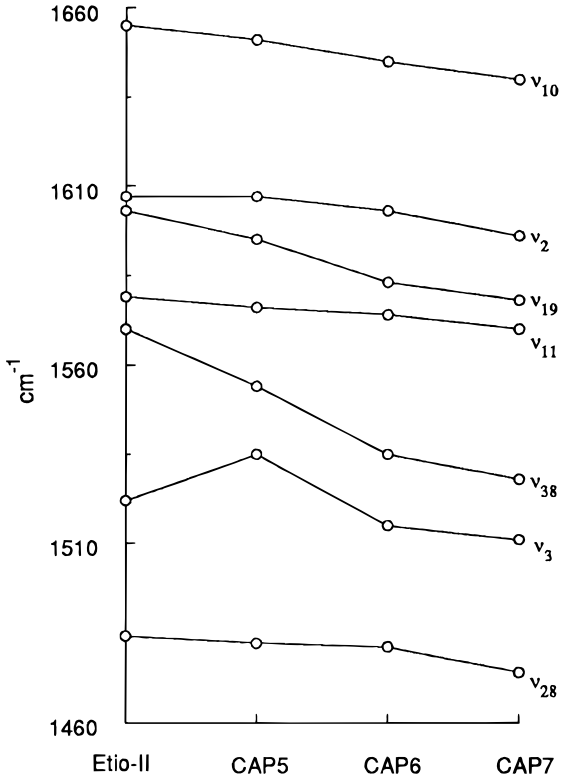

Figure 10. Graph showing that increasing size of the exocyclic ring in NiCAPs shifts structure-sensitive modes down in frequency.

Similar to NiEtios and NiTHBPs, the RR spectra of NiCAPs in the midrange (600−1200 cm^{-1}) with 568.2-nm excitation wavelength display a rich array of distinctive skeletal and peripheral bands, many of which can be used to determine cycloalkano ring size. Specific marker bands in the 1120−1200-, 880−900-, and 580−620-cm^{-1} regions, attributed to C_β−C and C−C stretching and deformational modes of the exocyclic ring, have been identified. The uniquely characteristic frequencies and variations of these modes offer valuable vibrational probes of structure for the NiCAP family.

Acknowledgment. This work was supported by the University of Houston President's Research and Scholarship Fund (PRSF) and in part by Grant E−1184 from the Robert A. Welch Foundation (to R.S.C). T.D.L. acknowledges support from the National Science Foundation under Grant No. CHE-9201149. Receipt of a Texaco Graduate Research Fellowship (J.G.R.) is gratefully acknowledged. We also thank Drs. T. G. Spiro and S. Hu (Princeton University) for making IR and normal mode analysis data of NiEtio-I available prior to publication.

IC950749O